

8p

1995/08/17
324757

N95-14531

Oscillatory/Chaotic Thermocapillary Flow Induced by Radiant Heating

Kwang-Chung Hsieh, † Robert L. Thompson, and David Van Zandt *
NASA Lewis Research Center
Cleveland, OH 44135

Kenneth DeWitt, and Jon Nash
The University of Toledo
Toledo, OH 44606

Abstract

The objective of this paper is to conduct ground-based experiments to measure the onset conditions of oscillatory Marangoni flow in laser-heated silicone oil in a cylindrical container. For a single fluid, experimental data are presented using the aspect ratio and the dynamic Bond number. It is found that for a fixed aspect ratio, there seems to be an asymptotic limit of the dynamic Bond number beyond which no onset of flow oscillation could occur. Experimental results also suggested that there could be a lower limit of the aspect ratio below which there is no onset of oscillatory flow.

I. Introduction

Surface tension driven convection (STDC) and its instabilities have been a subject of great interest in recent years. The microgravity environment provided by the space shuttle allows detailed study of the flow phenomena without the interference of the effect of buoyancy forces. In terms of the relative direction between the temperature and the surface tension gradients, instability of STDC can be divided into two categories, namely the B'énard-Marangoni (BMI) and the Marangoni flow instabilities. The B'énard-Marangoni flow is established by a temperature gradient normal to a liquid-liquid or a liquid-gas interface (heated from the bottom of the container). Infinitesimally small disturbances grow and develop into a steady state flow pattern when the Marangoni number exceeds a critical value for the first transition. This is recognized as the famous B'énard cell¹ in a thin liquid layer. Higher transitions to oscillatory and chaotic flows are being studied but are still in the exploratory stage^{2,3}.

As opposed to the B'énard - Marangoni flow instability (BMI), Marangoni flow starts once there is a temperature gradient established along the free surface such that there is no first transition. For higher flow transition, a Hopf bifurcation similar to that in the BMI could exist in this configuration. Transition from steady state to oscillatory flow has been observed in experiments with various container geometries.^{4,5,6} The possibility of further flow transition to the chaotic mode (second transition) at a higher Marangoni number (Ma) has not yet been well studied. Basically, two configurations have been adopted by various researchers to study the Marangoni flow instabilities. One is a floating zone and the other is an open-top container (square or cylindrical) filled with liquid. The floating zones are vertical liquid columns held between two cylindrical rods.

In the floating-zone configurations, Schwabe et al.⁷ concluded that the oscillatory state of thermocapillary flow is a distortion of the laminar state in the form of a wave travelling in the azimuthal direction. Napolitano et al.⁸ conducted float zone experiments on the Spacelab-D1 mission. This was the first microgravity experiment where large liquid bridges were produced, the largest being 6 cm in diameter and 8 cm in length. However, the oscillatory flow results were inconclusive. Vargas et al.⁹ observed thermocapillary flow oscillations for hexadecane, Fluorinert, and methyl alcohol test fluids in a simulated float zone configuration. Critical temperature differences for the onset of oscillations and the resulting frequencies of oscillation were determined for several aspect ratios. It was found that the critical Marangoni number is not the proper dimensionless parameter to describe the onset of oscillation. It was also shown that the oscillation mechanism is not in the form of an azimuthal travelling wave. Instead, once the oscillation appeared, a pair of vortices grew and decayed alternately in a cross-sectional (vertical) plane. Based on the phase shifts of the thermocouples, Velten et al.^{10,11} concluded that there are

† NYMA, Inc.

* ADF, Inc.

three discernable spatiotemporal structures of oscillatory convection. These are azimuthal running waves, axial running waves with a symmetric wave front, and axial running waves with a deformed wave front. Chun¹² and Velten¹⁰ both reported experimental results on time-dependent (oscillatory and turbulent) thermocapillary flow under microgravity and normal gravity conditions for simulated floating zone configurations. The latter stated that gravity had a more pronounced effect on the transition from oscillatory to turbulent flow.

Compared to the effort on float-zone configurations, fewer studies have been done on square or cylindrical container configurations. Lee¹³ conducted a normal gravity experimental study in a modified two-dimensional square cavity. One side wall was heated and the other one was maintained at room temperature. It was found that beyond a critical temperature difference between the side walls, an oscillatory flow phenomenon occurred. The conclusion was made that the oscillatory flow was caused by a Kelvin-Helmholtz type instability in the shear layer. In contrast to the square container, thermocapillary flow in a cylindrical container was also studied by Lee¹⁴ at normal gravity with a heating wire placed along the center axis. Oscillatory flow was observed in this configuration and it was concluded that the oscillation was caused by a coupling of the flow and the surface (capillary) waves.

Several models or mechanisms have been proposed to predict the onset of oscillations for "float-zone configurations". Chun's¹⁵ proposed model is that oscillations start if the maximum steady state heat flux occurs at the zero axial temperature gradient location on the interface. The origin of the oscillatory Marangoni instability was identified as a travelling wave of temperature perturbations on the free surface around the circumference of the floating zone. According to this model, the critical Marangoni number for the onset of oscillatory flow depends only on the aspect ratio (regardless of the size of the floating zone) for a typical fluid. To better characterize the onset phenomenon, a model by Ostrach¹⁶ states that there are two conditions to be satisfied in order for oscillations to begin. The first is that the critical Marangoni number must be exceeded and the second is that the critical value of the S-parameter (Capillary number/Prandtl number) must also be exceeded. Ostrach's model suggests that surface deformation (the S-parameter) plays a decisive role in the onset of oscillation.

In the present investigation, the flow configuration (shown in Fig. 1) is based on a cylindrical container filled with silicone oil. The temperature

gradient is established by directing a CO₂ laser on to the center of the free surface. The objectives of the present paper are to conduct ground-based experiments to measure the onset conditions of oscillatory flows, to formulate linear stability analysis to predict the onset conditions, and to characterize the onset of oscillatory thermocapillary flows using appropriate system parameters.

According to the previous research findings based on the floating zone configuration, for a typical fluid, the onset of flow oscillation can not be characterized by only one system parameter such as the aspect ratio (e.g., Chun's¹⁵ model). To better characterize the onset conditions of flow oscillations, a modified dynamic Bond number (in addition to the aspect ratio) is proposed (Section IV) in this paper. It is assumed that gravity always plays a role in the Marangoni instability due to the buoyancy force and the influence on the surface deformation.

The modified dynamic Bond number (Bo_{md}) here is defined as

$$Bo_{md} \equiv \frac{Ra^{r_1}}{Ma} Ca^{r_2} = \left(\frac{\rho g \beta \Delta T H^3}{\nu \alpha} \right)^{r_1} \left(\frac{\gamma \Delta T R}{\mu \alpha} \right)^{-1} \left(\frac{\gamma \Delta T}{\sigma} \right)^{r_2} \quad (1)$$

where Ra is the Rayleigh number, Ca is the Capillary number, H is the liquid height, R is the chamber radius, σ is the surface tension between silicone oil and air, $\gamma = -\frac{d\sigma}{dT}$, ρ is the density, α is the thermal diffusivity, ν is the kinematic viscosity, β is the thermal expansion coefficient, g is the gravity level, and $\Delta T = \frac{Q}{2\pi H k}$. Q is the total laser power and k is the thermal conductivity of silicone oil. The definition of ΔT is obtained by equating the input laser power to the total heat loss to the cooling water through the side wall. It is noted that the liquid height is chosen as the length scale for the Rayleigh number. This is due to the fact that, at normal gravity conditions, stratified layers can be clearly observed when the liquid layer gets thicker (larger H). It is believed that the stratified layers tend to stabilize the flow and delay the onset of oscillations. Perhaps a more pronounced effect of buoyancy force on the onset of oscillations can be seen with the present definition of the Rayleigh number.

In order for Bo_{md} to be a system parameter, the total exponential power for ΔT has to be zero. Thus the ΔT_c (or Q_c , the critical laser power) only appears in the critical Marangoni number as an output of the experiment. The above condition results in $r_2 = 1 - r_1$. For a single fluid, if the ratio of the laser beam diameter to the chamber diameter (r_{lc}) is fixed, the only variables in the system

are the gravity level, the chamber diameter, and the chamber height (three degrees of freedom). When the dimensions (diameter and height) of the chamber are selected, experiments conducted at various gravity levels will determine r_1 . According to the definition of Bo_{md} ,

$$Bo_{md} \propto g^{r_1} \cdot H^{3r_1-1} \left(\frac{H}{R}\right)^{-1}$$

Ideally, one could fix the aspect ratio ($Ar \equiv \frac{H}{R}$) and vary the size of the container until same critical Marangoni numbers are found at normal and micro-gravity levels. If the Bo_{md} is the appropriate nondimensional number for characterizing the onset conditions of the oscillatory flows, the r_1 can be determined and experimental data will be well correlated.

Currently, since almost no microgravity experimental data are available, the data in this paper will be presented using $r_1 = 1$ for simplicity (i.e., $Bo_{md} = \frac{Ra}{Ma}$).

II. Experimental Apparatus and Procedure

The apparatus used for the present experiment is shown in Fig. 2. It consists of: a cylindrical copper test chamber which contains the test fluid (2 cs. silicone oil) and has an adjustable Teflon bottom; a CO₂ laser system which serve as the radiant energy source to establish a temperature gradient and thus a surface tension gradient on the fluid surface which causes fluid movement; a Ronchi imaging system focused on the the fluid surface to insure leveling of the surface; an infrared imager to measure the temperature distribution on the fluid surface; a controlled water bath to provide a constant chamber wall temperature; thermistors embedded in the test chamber to record the wall temperature; a laser power meter; and direct data acquisition hardware. The test apparatus was assembled on an automatically-leveling optical table in order to eliminate any vibrations.

All experiments were conducted with a Gaussian distribution of laser beam intensity directed normal to the fluid surface and a beam ratio (the ratio of the laser beam diameter to chamber diameter) equal to 0.2. The chamber wall temperature was kept constant at 20° C. The parameters that were varied in the experiments are the aspect ratio, defined as $Ar = \frac{H}{R}$, where H is the fluid height and R is the chamber radius; and the dynamic Bond number, which is the ratio of the Rayleigh number to the Marangoni number, and is defined as

$Bo_{md} = \frac{\rho g \beta H^3}{\gamma R}$. In the present experiments, there are five chambers of various diameters (0.5, 1.0, 1.2, 2.0, 3.0 cm). The bottom wall of the test chambers are adjustable to accommodate various aspect ratios. Tests were conducted for constant aspect ratio and constant dynamic Bond number cases. The test matrix is as follows:

Constant Ar Cases: 0.5, 0.67, 0.8, 1.0, 1.2, 1.5, 2.0

Constant Bo_{md} Cases: 0.17, 0.34, 0.7, 1.0, 2.0

The thermodynamic and transport properties for 2 cs. silicone oil are listed below.

$$\begin{aligned} \lambda &= 0.109 \frac{W}{m \cdot K}; & \gamma &= 8.5 \times 10^{-5} \frac{N}{m}; \\ \nu &= 2.0 \times 10^{-6} \frac{m^2}{s}; & \rho &= 872 \frac{Kg}{m^3}; \\ \alpha &= 7.27 \times 10^{-8} \frac{m^2}{s}; & \beta &= 1.17 \times 10^{-3} \frac{1}{K} \end{aligned}$$

All of the electronic equipment was allowed to come to thermal equilibrium before the experiment were conducted. The laser was directed onto the fluid surface and a steady axisymmetric thermocapillary flow is developed. The laser power was then gradually increased in small increments until the flow became unstable and oscillatory. At the critical point for the onset of oscillatory motion, determined from the infrared image and/or the Ronchi imaging system, the laser power and the maximum temperature at the center of the fluid were measured. The experiment was then conducted starting from an oscillating fluid and the laser power was gradually decreased until oscillations ceased. Each test case was performed ten times and the average of these values was used to calculate the critical Marangoni number. Using the definition of ΔT in Eq. (1), the Marangoni number is defined as

$$Ma \equiv \frac{\gamma QR}{2\pi\mu\alpha kH} \quad (2)$$

III. Modeling and Numerical Analysis

To fully understand the surface tension driven flow instability, a theoretical investigation has to be conducted in parallel with the experimental study. Such analytical or numerical solutions to the problem can provide more detailed information which could help analyze and explain the measured data.

All theoretical studies on the stability limit for STDC were based on the float-zone configuration. No formal investigations have been performed for the flow configuration used in the present study. In the category of linear stability study on a float zone, neutral curves for hydrothermal waves with an assumed velocity profile at the basic state have been

presented by Smith and Davis¹⁷. In the second part of the article,¹⁸ they include the mechanism of free surface waves. However, their results are valid only for an infinite layer and do not compare well with experimental data. This is due to the fact that the effect of finite boundaries strongly alters the stability limit. To remedy this deficiency, Neitzel et al.¹⁹ applied the energy-stability theory to investigate the stability properties of thermocapillary convection in a float zone. In their study, the flow velocity at the basic state is obtained by solving the Navier-Stokes equations for incompressible flow. The calculated critical Marangoni numbers as a function of aspect ratio are in reasonable agreement with measured data⁴, but the free surface deformation effect is not included. Lai et al.²⁰ have shown the importance of free surface deformation on the onset of oscillatory flow. They concluded that the time lag between velocity and temperature due to the surface deformation controls the onset of oscillation. However, their conclusion was drawn without any consideration of the effect of hydrodynamic instability. Hence, a stability analysis with a full account of hydrothermal waves and free surface waves in a finite domain is necessary to advance the understanding of the problem. A linear stability analysis is proposed in this section. The solutions for the basic state will be obtained using a numerical method by solving the Navier-Stokes equations with free surface deformation.

The evolution of disturbances in STDC is governed by the incompressible Navier-Stokes equations with the Boussinesq approximation:

$$\nabla \cdot \vec{V} = 0 \quad (3)$$

$$\frac{\partial \vec{V}}{\partial t} + (\vec{V} \cdot \nabla) \vec{V} = -\frac{1}{\rho_o} \nabla p - \nabla \times [\nu (\nabla \times \vec{V})] + \nabla [2\nu \nabla \cdot \vec{V}] + \beta(T - T_o) \vec{g} \quad (4)$$

$$\frac{\partial T}{\partial t} + (\vec{V} \cdot \nabla) T = \nabla \cdot (\alpha \nabla T) + \frac{1}{\rho_o c_p} \left[\frac{\partial p}{\partial t} + (\vec{V} \cdot \nabla) p \right] \quad (5)$$

where \vec{V} is the velocity vector, ρ_o is the density at a reference temperature T_o , p is the static pressure, T is the temperature, c_p is the specific heat at constant pressure, and \vec{g} is the gravity vector.

In this paper, we formulate the incompressible stability problem in cylindrical coordinates for the present configuration. The total field can be decomposed into a mean value and a perturbation quantity:

$$\phi = \bar{\phi} + \phi' \quad \text{and} \quad \phi = (p, u, v, w, T)^T \quad (6)$$

where u is the velocity component in the radial direction, v is the velocity component in the tangential direction, and w is the velocity component in the axial direction.

Following the linear theory, we assume that the disturbance vector ϕ for an instability wave with an azimuthal wave number m can be expressed as

$$\phi'_{(r,\theta,z,t)} = \Psi_{(r,z)} e^{im\theta - \lambda t} \quad (7)$$

where λ is the eigenvalue of the system and Ψ is the "shape function" vector given by

$$\Psi = (\hat{p}, \hat{u}, \hat{v}, \hat{w}, \hat{T})^T \quad (8)$$

It is noted that a harmonic solution is assumed in the θ direction with a wavenumber m . This is because in the ground-based experiment, the oscillatory flow exhibits standing-wave structure in the azimuthal direction. Based on this phenomenon, it is assumed that the onset of flow oscillations is mainly triggered by the growth of azimuthal disturbance. With the formulation in Eq. (7), the system of equations is reduced to a two-dimensional form and more efficient numerical calculations can be carried out. For linear stability analysis, a single disturbance mode (m) is considered.

Substituting Eq. (6) into Eqs. (3)-(5), subtracting the perturbation equation from the governing equations corresponding to the steady mean flow, linearizing the perturbation equation, and using Eqs. (8)-(9) give the following equations for the shape function

$$\hat{A} \frac{\partial \Psi}{\partial r} + \hat{C} \frac{\partial \Psi}{\partial z} + \hat{D} \Psi = V_{rr} \frac{\partial^2 \Psi}{\partial r^2} + V_{rz} \frac{\partial^2 \Psi}{\partial r \partial z} + V_{zz} \frac{\partial^2 \Psi}{\partial z^2} \quad (9)$$

where the vectors \hat{A} , \hat{C} , and \hat{D} are defined as

$$\hat{A} \equiv A - imV_{r\theta}$$

$$\hat{C} \equiv B - imV_{z\theta}$$

$$\hat{D} \equiv -\lambda\Gamma + D + imB + m^2V_{\theta\theta}$$

Matrices Γ , A , B , C , D , V_{rr} , $V_{r\theta}$, V_{rz} , $V_{\theta\theta}$, $V_{\theta z}$, and V_{zz} are Jacobians of the corresponding total flux vectors. For linearized perturbation equations, they contain only mean flow quantities. The mean flow quantities are obtained by solving the steady state Navier-Stokes equations in the (r, z) coordinate system numerically.²¹ The eigenvalue problem given by Eq. (9) can then be solved by following the technique of Malik.^{22,23} The solutions gives the neutral stability curve at which γ is a purely imaginary number.

IV. Discussion of Results

Based on the test matrix given in Section II, the critical Marangoni numbers have been measured for each test condition in which the onset of flow oscillation occurs. Figure 3 shows the measured critical Marangoni number (Ma_c) versus dynamic Bond number (Bo_{md}) at various aspect ratios. In general, the Ma_c increases with Bo_{md} . This can be attributed to the stabilization effect of the stratified layer caused by gravity. According to Fig. 3, for each aspect ratio (Ar), there seems to be an asymptotic limit of Bo_{md} beyond which there is no onset of oscillation. The effect of Ar on the onset of oscillations can be seen in Fig. 4. For small aspect ratios, while the effect of the stratified layer is reduced, the bottom wall starts to play a dominant role in the onset of oscillations. Due to the wall damping, a higher laser power is needed to make the fluid unstable. As shown in Fig. 4, the critical Marangoni numbers increase sharply when aspect ratios are lower than 0.5. It seems that there exists a lower limit of Ar below which there is no onset of oscillations. In Fig. 4, it can be seen that when Ar is greater than 0.8, the critical Marangoni number approaches a constant and becomes insensitive to the dynamic Bond number. This might suggest that for a deep layer, the characteristics of the onset of oscillations on earth are quite close to those in the microgravity environment.

In the present study, the onset of oscillations is characterized using two system parameters: Ar and Bo_{md} . A stability map can be generated as shown Fig. 5. In the test matrix, there are a number of cases at which no onset of oscillations can be observed. These points can roughly determine the domain of instability. It is noted that in a part these nonoscillating cases, the laser power was so high such that significant evaporation of the silicone oil occurred. This might have altered the characteristics of the onset of oscillatory flows.

V. Conclusion

A series of ground-based experiments have been conducted to measure the onset conditions of the oscillations of Marangoni flows based on 2 cs. silicone oil in a cylindrical container heated with CO₂ laser. For a single fluid, in addition to the aspect ratio, a modified dynamic Bond number (a combination of capillary and traditional dynamic Bond number) is proposed to correlate the experimental data. Results obtained from ground-based experiments show that for each aspect ratio there seems to

be an asymptotic limit for the dynamic Bond number beyond which no flow oscillations could occur. On the other hand, for each dynamic Bond number, a lower limit of the aspect ratio seems to exist for the onset of flow oscillations.

References

1. B'enard, H., *Rev. Gev. Sci. Pure Appl.*, vol. 11, pp.1261-1271, 1309-1328, 1990.
2. Koschmieder, E. L., and Pallas, S. G., *Int. J. Heat Mass Transfer*, vol. 22, pp. 535-546, 1974.
3. Davis, S. H., "Thermal Capillary Instabilities," *J. Ann. Rev. Fluid Mech.*, vol. 19, pp. 403-435, 1987.
4. Velten, R., Schwabe, D., and Scharmann, A., "The Periodic Instability of Thermocapillary Convection in Cylindrical Liquid," *Phys. Fluids A*, vol. 3, No. 2, pp. 267-279, 1991.
5. Ostrach, S., Kamotani, Y., and Lai, C. L., "Oscillatory Thermocapillary Flows," *Phys. Chem. Hydro.*, vol. 6, No. 5/6, pp. 585-599, 1985.
6. Monti, R., and Fortezza, R., "Oscillatory Marangoni Flow in a Floating Zone: Design of a Telescience Experiment for Texas 23," Proceedings of the 7th European Symposium on Materials and Fluid Sciences in Microgravity, pp. 285-289, 1989.
7. Schwabe, A. and Scharmann, A., "Measurements of the Critical Marangoni Number of the Laminar Oscillatory Transition of Thermocapillary Convection in Floating Zones," ESA SP-222, p. 281, 1984.
8. Napolitano, L. G., Monti, R., and Russo, G., "Some Results of the Marangoni Free Convection Experiment," ESA SP-222, p. 15, 1984.
9. Vargas, M., Ostrach, S., and Kamotani, Y., "Surface Tension Driven Convection in a Simulated Floating Zone Configuration," M. S. Thesis, Dept. of Mech. and Serospace Engr., Case Western University, 1982.
10. Velten, R., Schwabe, D., and Scharmann, A., "Gravity-Dependence of the Instability of Surface-Tension Driven Flow in Floating Zones," ESA SP-295, p. 271, 1989
11. Velten, R., Schwabe, D., and Scharmann, A., "The Periodic Instability of Thermocapillary Convection in Cylindrical Liquid Bridges," *Phys. Fluids*, A3, p. 267, 1990.

12. Chun, C. H., "Verification of Turbulence Developing from the Oscillatory Marangoni Convection in a Liquid Column," ESA SP-222, p.271, 1984.
13. Lee, K., "An Experimental Study of Combined Natural and Thermocapillary Convection in a Rectangular Container," M. S. Thesis, Dept. of Mech. and Aerospace Engr., Case Western Reserve University, 1986.
14. Lee, J. H., "An Experimental Study of Thermocapillary Convection in a Cylindrical Container," M. S. Thesis, Dept. of Mech. and Aerospace Engr., Case Western Reserve University, 1990.
15. Chun, C. H., "Experiments on Steady and Oscillatory Temperature Distribution in a Floating Zone Due to the Marangoni Convection," *Acta Astronautica*, 7, p. 479, 1980.
16. Ostrach, S. and Kamotani, Y., "Recent Developments in Oscillatory Thermocapillary Flows," AIAA/IKI Microgravity Science, Conference Proceedings, p. 25, 1991.
17. Smith, M., and Davis S., "Instabilities of Dynamic Thermocapillary Liquid Layers, Part 1. Convective Instabilities," *J. Fluid Mech.*, vol. 132, pp. 119-144, 1983.
18. Smith, M., and Davis S., "Instabilities of Dynamic Thermocapillary Liquid Layers, Part 2. Surface-Wave Instabilities," *J. Fluid Mech.*, vol. 132, pp. 145-162, 1983.
19. Neitzel, G. P., Law, C. C., Jankowski, D. F., and Mittelman, H. D., "Stability and Instability of Thermocapillary Convection in Models of Float-Zone Crystal Growth," *AIAA J.*, pp. 57-65, 1991.
20. Lai, C. L., Ostrach, S., Kamotani, Y., "The Role of Free-Surface Deformation in Unsteady Thermocapillary Flow." Japan Heat Transfer Joint Seminar, San Diego, California, September 17-20, 1985.
21. Hsieh, K.-C., and Pline, A. D., "A Comprehensive Numerical Study of Surface Tension Driven Convection with Free Surface Deformation," AIAA Paper No. 91-1306, 26th Thermophysics Conference, June, 1991.
22. Malik, M. R., "A Numerical Methods for Hypersonic Boundary Layer Stability," *J. Computational Physics*, Vol. 86, No. 2, pp. 376-413, 1990.
23. Malik, M. R., Chuang, S., and Hussaini, M. Y., "Accurate Numerical Solution of Compress-

ible Linear Stability Equations," *ZAMP*, Vol. 33, No. 2, 189., 1982.

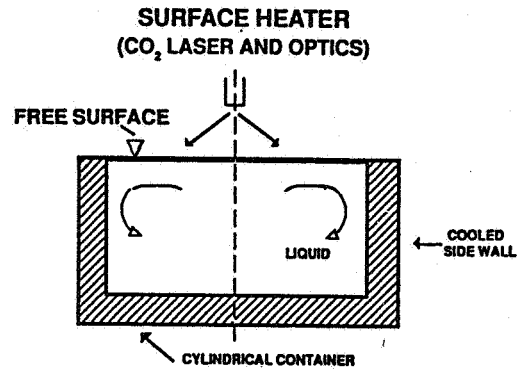


Fig. 1 Schematic Diagram for Flow Configuration

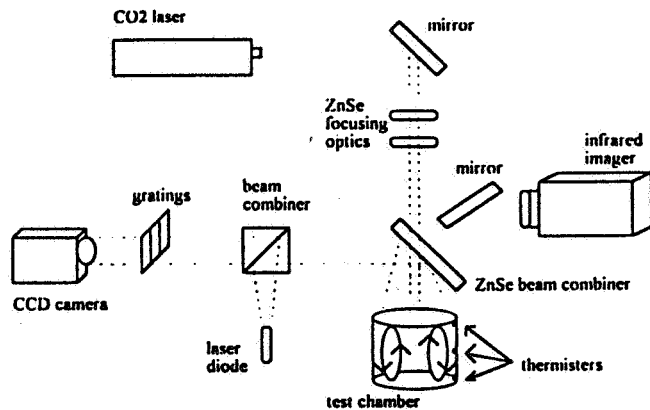


Fig. 2 Schematic Diagram for Experimental Setup

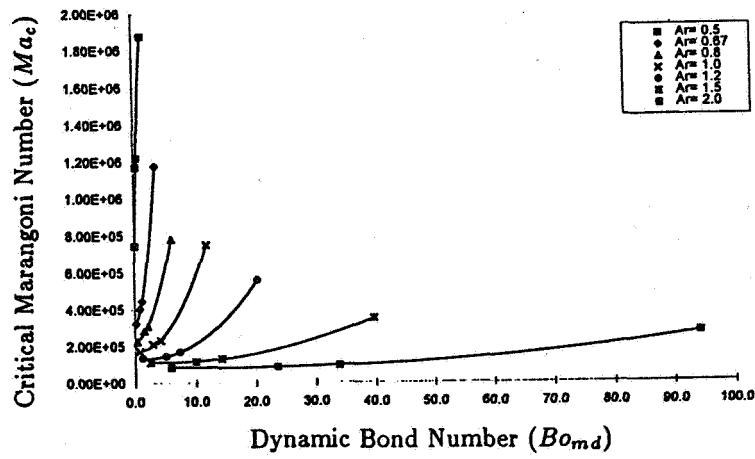


Fig. 3 Measured Critical Marangoni Number versus Dynamic Bond Number for Various Aspect Ratios

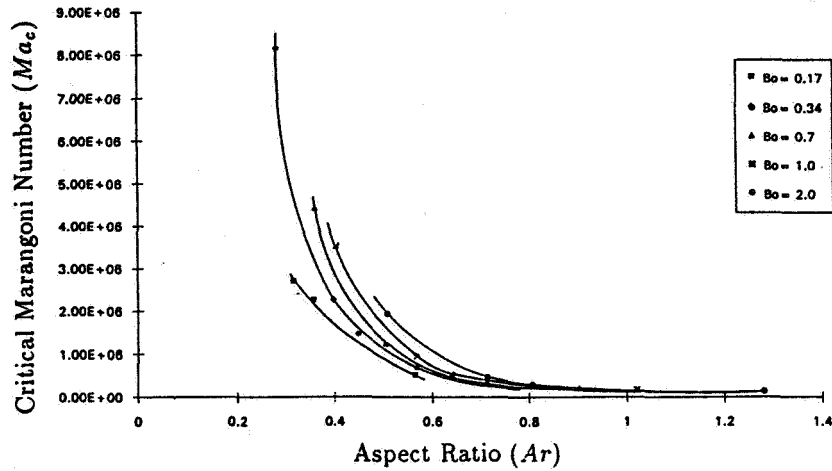


Fig. 4 Measured Critical Marangoni Number versus Aspect Ratio for Constant-Dynamic-Bond-Number Cases

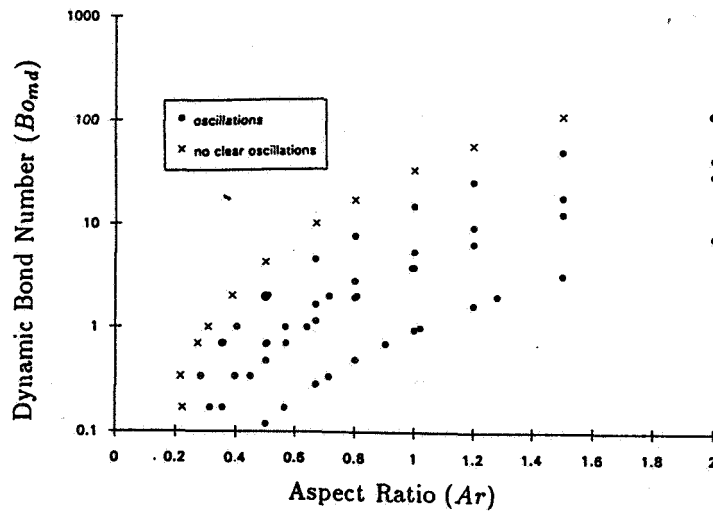


Fig. 5 Flow Instability Map Determined from Ground-Based Experiments